Environ. Sci. Technol. **1999**, *33,* 1286−1292

Surfactant Enhanced Perchloroethylene Dissolution in Porous Media: The Effect on Mass Transfer Rate Coefficients

JONATHAN C. JOHNSON, SHAOBAI SUN, AND PETER R. JAFFÉ*

Department of Civil Engineering and Operations Research, Princeton University, Princeton, New Jersey 08544

The effect of a surfactant on the mass transfer rate coefficient, *K*, during the dissolution of a nonaqueous phase liquid (NAPL) was investigated using batch and column experiments. Batch experiments were performed at several surfactant concentrations holding the interfacial area between perchloroethylene (PCE) and the surfactant solution constant. Porous media experiments were also conducted at the same surfactant concentrations and an unknown interfacial area to evaluate the effect of the surfactant on the mass transfer rate coefficient, *K*, during dissolution of PCE from residual saturation to zero saturation. The experimental results show the following: (1) The addition of surfactant at concentrations below its critical micelle concentration (CMC) yields almost no difference in mass transfer rate coefficient despite a 3-fold decline in surface tension. (2) Above surfactant CMC, the presence of surfactant reduces the mass transfer rate coefficient. (3) Though a decrease in mass transfer rate coefficient is found, there is an overall increase in mass transfer due to the higher driving force. (4) The amount of the change in mass transfer rate coefficient, above CMC, is roughly proportional to the normalized mass transfer rate coefficients found from batch systems with constant interfacial area. The similarity between the results from batch experiments and the porous media experiments yield a technique for prediction of the mass transfer rate coefficient in porous media without having to repeat a dissolution experiment in porous media for each surfactant concentration. Results from modeled simulations demonstrate that the effect of the surfactant on the mass transfer rate coefficient is an important factor. Predictions regarding surfactant enhanced dissolution need to include the effect of the surfactant on the mass transfer rate coefficient. Without the appropriate correction in the mass transfer rate coefficient, simulations will under predict the amount of time and effort required to remove nonaqueous phase liquids from the subsurface using this technology.

Introduction

Mass Transfer from Residual Phase NAPL. The dissolution of a nonaqueous phase liquid (NAPL) is described by a pair of coupled partial differential equations. The first equation describing the mass balance in the nonaqueous phase,

$$\phi\rho_n\frac{dS_n}{dt} = -K(C_s - C) \tag{1}$$

the second describing the mass balance in the aqueous phase (assuming 1-D flow).

$$\frac{\partial\theta_w C}{\partial t} = D\frac{\partial^2 C\theta_w}{\partial x^2} - v\frac{\partial\theta_w C}{\partial x} + K(C_s - C) \tag{2}$$

here, C is the concentration in the aqueous phase, C_s is the solubility limit for the NAPL, K is the mass transfer rate coefficient [T^{-1}], S_n is the NAPL saturation, ρ_n is the NAPL density, ϕ is the porosity, θ_w is the volumetric water content (volume of water per unit volume of porous media), D is the hydrodynamic dispersion coefficient, and v is the average linear velocity. This pair of equations is coupled by the term $K(C_s - C)$ which describes the rate of transfer of mass between the two phases.

Dissolution is discussed as a cleanup method in early papers on the subject of nonaqueous phase pollution problems (*1*−*3*); however, these works did not specifically focus on the mass transfer process. A later work more thoroughly describes this mass transfer from the nonaqueous phase to the aqueous phase (*4*), giving treatment to the conceptual model used for mass transfer, and the mathematical model employed from a dimensional analysis perspective. For mass transfer in porous media a stagnant film model of dissolution across an interface is employed. In the region of the aqueous-phase stagnant film, the flux of the organic constituent from the organic phase to the bulk liquid is described via molecular diffusion across this film with a thickness of δ. Mathematically the dissolution is expressed as the diffusive flux from an organic phase across the stagnant film into the bulk aqueous phase.

$$\frac{1}{V}\frac{dm}{dt} = \frac{D_m}{\delta}\frac{A}{V}(C_s - C) \tag{3}$$

here, V is the system volume (for porous media it is the volume of porous media); m is the mass of dissolved contaminant; D_m is the molecular diffusion coefficient for the contaminant in the aqueous environment; A is the interfacial area; C_s is the solubility limit; and C is the concentration in the bulk aqueous phase; and δ is the thickness of the film. The ratios D_m/δ and A/V are often renamed k, the mass transfer coefficient, and a, the specific interfacial area, respectively. Further combination results in a lumped parameter K, where $K = ka$, and K is known as the mass transfer rate coefficient, the same coefficient seen in eqs 1 and 2.

Experimental work has been performed to relate mass transfer rate coefficients in porous media to particle size and pore geometry (*4*−*7*), flow rate (*4*−*5, 7*−*9*), saturation (*4*−*5, 7*−*9*), and NAPL composition (for a two component NAPL mixture) (*7*). Most of these investigators have utilized effluent measurements to obtain "average" mass transfer rate coefficients over the length of their column (*4*−*7, 10*). One investigator used a gamma radiation attenuation technique to measure column saturation at discrete locations along the column, yielding detailed spatial and temporal data along the column axis (*8*−*9*).

The Role of Surfactants in Mass Transfer. The dissolution rate of a NAPL in a porous medium is described by the three components of the mass transfer equation: (1) the driving force, given by the gradient in concentration, which drives

* Corresponding author phone: (609)258-4653; fax: (609)258-2799; e-mail: jaffe@ceor.princeton.edu.

10.1021/es980908d CCC: $18.00 © 1999 American Chemical Society
Published on Web 03/11/1999

diffusion; (2) the mass transfer coefficient, k; (3) and the specific interfacial area, a. Surfactants are expected to impact each of these three components of the mass transfer from the NAPL to the aqueous phase.

Surfactants are organic molecules with different end portions (moieties). One end of the molecule is distinctly hydrophilic, while the other one is hydrophobic. The hydrophilic moiety allows the surfactant to be soluble in water, while the hydrophobic moiety is more soluble in a nonpolar environment. The most energetically favorable position for such a molecule is at the interface between the aqueous phase and a nonaqueous phase. In the vadose zone that may mean they accumulate at the interface between water and the vapor phase, or between the water and natural organic carbon, attached to the soil. For two-phase systems of water and NAPL, the surfactant molecules will accumulate at the interface between the two fluids. The accumulation of surfactant molecules at an interface tends to lower the interfacial tension. Thus, the addition of surfactants to a NAPL water system makes it easier to create additional interfacial area between the two fluids.

Once the available interface has become sufficiently covered by surfactant, self-organization of the surfactant in solution into energetically favorable geometries occurs. In solution the surfactant molecules tend to form clusters, or micelles (with the hydrophobic moieties all in close proximity and the hydrophilic moieties pointing toward aqueous solution), with geometries of spheres, rods, or sheets depending on the surfactant concentration. The surfactant concentration at which this self-organization begins is referred to as the critical micelle concentration or CMC. The CMC is actually a range of concentrations over which different organizational patterns are possible. Above CMC the self-organized surfactant micelles have the capacity to partition low-solubility organic compounds from the aqueous phase into their core. Thus the apparent solubility of some organic compounds can be increased by the addition of surfactants above their CMC (*11, 12*). The apparent aqueous phase concentration of a low solubility hydrocarbon is defined as the sum of the truly dissolved phase plus the phase that is partitioned into the aqueous surfactant micelles.

Laboratory experiments involving the solublization and/or mobilization of dense nonaqueous phase liquid (DNAPL) by surfactant solution have focused on high surfactant concentrations. This results in either mobilization of the DNAPL (*13*) or enhanced dissolution (*14*−*16*). In either case the surfactant concentration tends to be very high and the interfacial tension very low and may have the tendency to form macroemulsions. This causes concern for two reasons: First, no studies have as yet determined the behavior of the small separate phase droplets that result from mobilization. Second, the formation of macroemulsions is not necessarily a favorable condition for the cleanup process. Macroemulsions could be expected to behave as solids in the porous media (*16*) and may thereby plug flow paths, possibly reducing the local permeability to water flow.

The emphasis on high concentration of surfactants has focused on the ability of surfactants to increase the driving force for dissolution by increasing the soluble limit of the contaminant (*14*−*16*). Additional attention has been paid to the possibility for mobilization due to reduced surface tension (*13, 15, 17*). The effect of surfactants on the mass transfer rate coefficient, K, has received scant attention in the literature (*18*). The arrival of surfactants at the interface might be expected to affect the mass transfer coefficient, k, by changing the properties of the interface, or alter interfacial area, a, by changing the stable configuration of the interface. An effect on either the mass transfer coefficient or on the interfacial area translates into a direct effect on the mass transfer rate coefficient. The effect of surfactants on the mass transfer coefficient, k, has been explored for the case of surfactant enhanced biodegredation by Guha and Jaffé (*19*). They give both experimental evidence and theoretical justification for a decreasing mass transfer coefficient with surfactant concentration above the surfactant CMC for a low solubility hydrocarbon.

TABLE 1. Properties of PCE in the Presence of Surfactant Solution

surfactant concn Triton X-102 (mg/L)	PCE solubility (mg/L)	interfacial tension (dynes/cm)	normalized mass transfer coeff from batch reactor, k_b/k_0
0	240	43.3	1.0
25	240	21.6	0.92
50	240	17.5	0.96
200	260	14.5	0.95
500	350	11.7	0.84
1000	590	7.2	0.61

This work addresses the behavior of the mass transfer rate coefficient between the aqueous and the nonaqueous phase in the presence of a surfactant during the dissolution of a residual NAPL phase in a porous medium. Two kinds of experiments are reported here: batch experiments that measure the mass transfer rate coefficient, K, when the interfacial area is known, and porous media experiments in a column, which measure K when the interfacial area is unknown. Data from the batch experiments are used to analyze the results of the column experiments.

Materials and Methods

Materials. The DNAPL chosen was perchloroethylene (PCE) $Cl_2C{=}Cl_2C$ which has a density of 1.63 g/cm^3. A nonionic surfactant, Triton X-102, which is commonly described as an alkylaryl polyether alcohol $(CH_3)_3CCH_2C(CH_3)_2C_6H_4(OCHCH)_n$-OH, was chosen for these experiments. The hydrophilic moiety of this surfactant has an average chain length, n, of 12.5. The critical micelle concentration for this surfactant is at about 150 mg/L measured using interfacial tension between the surfactant solution and the PCE. The CMC may appear at a slightly different concentration depending on the property from which it is inferred. The selection of this surfactant was based on preliminary screening using the batch technique and on interfacial tension measurements; the intent was to achieve enhanced solubility without inducing mobilization or emulsification of the PCE.

The interfacial tension of PCE and surfactant solution was determined using a Du Noy ring tensiometer. For deionized water the interfacial tension was found to be 43.3 dynes/cm. Table 1 gives the properties of PCE found for these column experiments and the effects of surfactants on their values.

The solubility of PCE is commonly reported as 150 or 200 mg/L at 25 °C (*20*−*22*). A reported PCE solubility value using a different procedure (*23*) is 237.0 mg/L at 25 °C (*24*). The value reported using the latter method is closer to the value established during these experiments. For PCE solubility in deionized water a value of 240 mg/L ± 10 mg/L was found for the column experiments conducted here.

Surfactants are typically mixtures of similar molecules having average properties. Selective partitioning of surfactants onto the surface can alter surfactant average properties. These experiments are conducted to minimize the effects of selective partitioning. Batch experiments are conducted after the surfactant solution and the PCE phase have equilibrated with large volumes of surfactant solution. Column experiments flush surfactant solution numbering in the thousands of pore volumes over the course of an experiment. In the

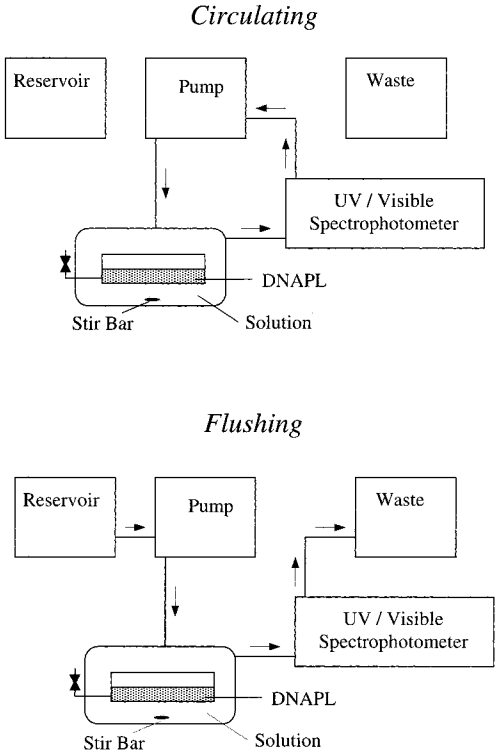

FIGURE 1. A sketch of the experimental setup for the batch dissolution experiments.

column experiments equilibration of the surfactant solution and the PCE is assumed to occur within the first few pore volumes, which comprise a very small fraction of the data. Partitioning to the porous media was low for this surfactant; breakthrough curves for the surfactant differed from the breakthrough of a conservative tracer by one-third of a pore volume.

Mass Transfer Coefficients from Batch Systems. To measure mass transfer rate coefficients in the presence of a surfactant, an apparatus allowing dissolution to proceed with a known interfacial area was constructed (*25*), thereby allowing calculation of the mass transfer rate coefficient under varying surfactant concentrations. The customized batch reactor is depicted in Figure 1. The apparatus consists of a short cylindrical glass plate in which the DNAPL is placed. The plate is suspended in and surrounded by a glass chamber of known internal volume. The glass chamber has three ports through which fluids can be injected or removed. The space below the glass plate allows for a magnetic stir bar, which provides for sufficient mixing without affecting the interfacial area.

The procedure for obtaining the mass transfer rate coefficient for a given surfactant concentration requires two stages of operation, circulating and flushing. First the chamber is entirely filled with the surfactant solution, removing all headspace air from the system, and then the DNAPL (PCE) is injected onto the glass plate. The circulation phase allows the system to be brought to equilibrium in order to determine the apparent aqueous-phase solubility of PCE in the presence of surfactant (C_E). The surfactant solution is circulated through the system in a closed loop. The effluent PCE concentration from the chamber is measured by a UV spectrophotometer at 235, 245, 255, and 277 nm and reinjected (multiple wavelengths are used in the measurement procedure to allow for subtraction of the spectrum due to the surfactant). After the spectrophotometric measurements indicate that steady-state PCE concentration, C_E, has been achieved (greater than 15 h) the valves are switched to begin the flushing stage.

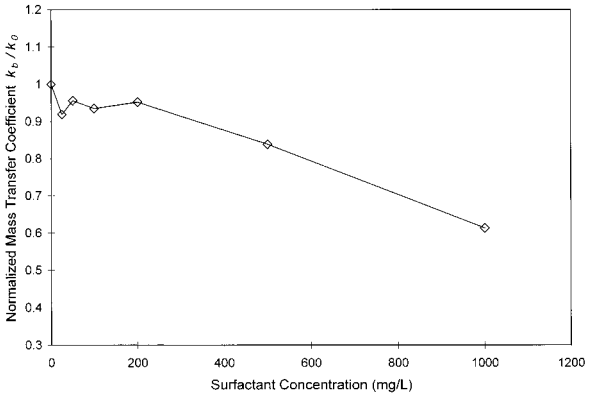

FIGURE 2. The effect of the Triton X-102 concentration on the normalized mass transfer coefficient during batch experiments.

During the flushing stage a fresh surfactant solution is pumped into the chamber at a known rate. The effluent is monitored for the dissolved PCE concentration. When the PCE concentration has again leveled off, a second steady-state concentration, C_F, is established.

The dissolved-phase PCE concentration in the reactor can be described as

$$V\frac{dC}{dt} = k_b A(C_E - C) - QC \qquad (4)$$

where C is the actual concentration of PCE in solution; C_E is the equilibrium solubility of PCE in solution; A is the area of the PCE-aqueous interface; V is the volume of the reactor; Q is the flow rate; and k_b is the mass transfer coefficient to be determined for this batch experiment. At steady state, $dC/dt = 0$, and, in the flushing stage, $C = C_F$, where C_F is the concentration reached at steady-state the end of the flushing stage. All three of these concentrations are apparent concentrations as defined above. This allows ready calculation of the mass transfer coefficient provided the interfacial area and the flow rate are known.

$$k_b = \frac{Q}{A} \cdot \frac{C_F}{C_E - C_F} \qquad (5)$$

Results from these batch experiments are found in Table 1.

Batch Reactor Results. A mass transfer coefficient, k_0, for the dissolution of PCE into pure water of 0.14 cm/min was obtained using the procedure outlined above. Mass transfer coefficients for dissolution of PCE into surfactant solution are reported here as normalized mass transfer coefficients, that is k_b/k_0. Figure 2 shows the k_b/k_0 value vs surfactant concentration. The results show that below the surfactant's CMC the concentration of surfactant has little effect on mass transfer coefficient. Above the CMC, increases in surfactant concentration result in a decrease in mass transfer coefficient. The method yields results reproducible to better than 5%; however, for this study not enough replicates were collected to report meaningful values of standard error.

Column Experiments. Sieved sand, a mixture of Ottawa F-75 and Federal Fine (U.S. Silica, Berkeley Springs, WV), was used for the column experiments. The sand was washed with deionized water, incinerated at 550 °C for at least 2 h, and then sieved using the U.S. standard sieve sizes, no. 30, no. 40, no. 50, no. 60, and no. 100. Sand passing the no. 100 sieve was discarded, and sand retained on the no. 30 sieve was discarded. The sand was then recombined by weight in the following recipe: no. 40 35.4%, no. 50 49.4%, no. 60 11.7%, and no. 100 3.5%, yielding a sand with a mean grain size of 0.39 mm. This procedure yields a reproducible, uniform sand

of known characteristics. Dry sand is packed into the column using a double-screened tube approximately a third of the diameter of the sand pack. This results in a uniform pack of relatively homogeneous porosity. The sand is supported at the bottom of the column by a steel screen covered by a Teflon mesh. Above the test sand is placed a filter sand and above that a very fine sand mixed with crushed silica of known properties. The filter sand consisted of incinerated Ottowa F-75 sand. The fine sand consisted of Ottowa F-75 sand mixed with 30% crushed silica (U.S. Silica sil-co-sil 90). The fine sand provides a capillary barrier for the emplacement of PCE.

The column is of aluminum construction and is 8.25 cm in diameter, it is machined to have a wall thickness of 1.02 mm (*9*), and has a height of 3.5 cm, in which about 20 mm of the testing sand is packed. The packed column typically contains a pore volume of approximately 60 mL. The rest of the column apparatus is made of thicker aluminum and has Viton O ring seals at four locations.

The experimental apparatus used is identical to that described in the literature for other mass transfer experiments without the presence of surfactants (*8, 9*). The only change is the addition of the UV/visible spectrophotometer to measure dissolved effluent concentrations of PCE and surfactant. The use of the spectrophotometer also allowed the effluent to be monitored for the presence of emulsions (not found in any of the experiments performed here).

A gamma radiation source−detector combination was used to measure nonaqueous phase PCE saturation in the column. The gamma radiation system consists of a source, Americium-241 embedded in a brass block with a horizontal lead collimator slit 1 mm high allowing radiation to pass through, and a detector, also equipped with a horizontal 1 mm lead slit. The gamma source and detector are precisely aligned along their 1 mm slits. The detector is a NaI crystal with an EG&G Ortec 276 photomultiplier tube. Data are collected from the photomultiplier by an EG&G Ortec 918 ADCAM multichannel buffer and stored on a computer.

To measure the PCE saturation in the column gamma radiation with a known energy level is directed through the column, and the attenuation of that energy is measured with the detector (*9, 26, 27*). The radiation is directed through the column as a 1 mm thick horizontal slice that is 2.8 cm wide at the front of the column and 4 cm wide at the rear (see Figure 3). PCE has a higher absorbance of gamma radiation per unit volume than water, which provides the needed contrast for measuring saturation with the gamma attenuation technique. With proper calibrations, and assuming the porosity does not change with time, a single energy gamma radiation source and detector combination can be used to determine the porosity and the saturation in a system with two fluid phases. This technique has advantages, such as the ability to measure saturation at discrete locations along the column, as opposed to measuring column average information. From these measurements of NAPL saturation along the longitudinal axis of the column and over time, mass transfer rate coefficients can be calculated as a function of column location and time (*8*).

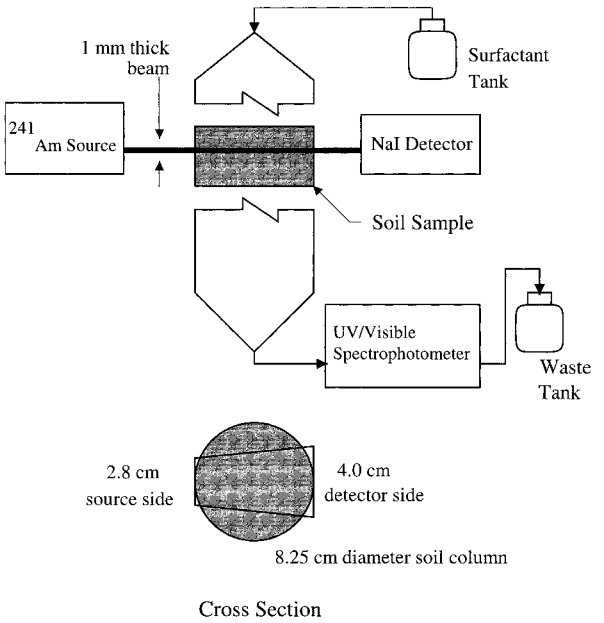

FIGURE 3. Experimental apparatus used to determine saturation in porous media. The setup here is identical to that used by other researchers (*8*), except for the addition of the UV/visible spectrophotometer.

The sand-filled column is mounted on an immobile rack between the source and detector of the gamma radiation system. The source/detector combination is mounted on a moving table which is capable of measuring vertical motion to 0.01 mm. Figure 3 shows the orientation of the gamma radiation equipment in relation to the sand filled column. The column is initially full of dry sand; it is then flushed with CO_2 and then filled with deionized water. After the column is water saturated, PCE is introduced from below by pumping under constant head at no more than 0.5 mL/min. Once the PCE saturation has gone above approximately 50%, water is pumped into the column from the top down, leaving behind PCE at residual saturation in the testing sand. After the chambers above and below the column have been rinsed free of PCE the dissolution portion of the experiment begins. Surfactant solution is pumped at approximately 2 mL/min into the column resulting in a darcy velocity of about 0.5 m/day. PCE saturation is measured at about 25 locations along the column. Using count times of approximately 5 min results in a standard error for saturation measurement of about 0.0024 (*8, 9*). This procedure allows each location to be measured during each experiment every 2−3 h, with an experiment lasting anywhere from 8 to 21 days. Flow rate was measured periodically throughout each experiment by timing the elution of 20 mL of effluent. Room temperature was controlled to be 21.0 ± 1.0 °C.

TABLE 2. Matrix of Experiments Performed[a]

experiment	surfactant concn (mg/L)	sand pack	av porosity	std dev porosity	av flow rate (mL/day)	av initial PCE saturation	total pore volumes flushed	percent mass removed (%)
Water1	0	A	0.344	0.014	2802	0.14	1200	98
Water2	0	D	0.326	0.001	2732	0.11	1475	97
T25	25	B	0.343	0.006	2690	0.14	1570	94
T50	50	A	0.344	0.014	2756	0.23	1120	96
T200	200	C	0.332	0.008	2681	0.15	1020	95
T500	500	D	0.326	0.001	2770	0.08	560	80
T1000	1000	A	0.344	0.014	2730	0.11	475	100

[a] Sand pack and porosity information based on those slices included in the analysis. Surfactant CMC is approximately 150 mg/L.

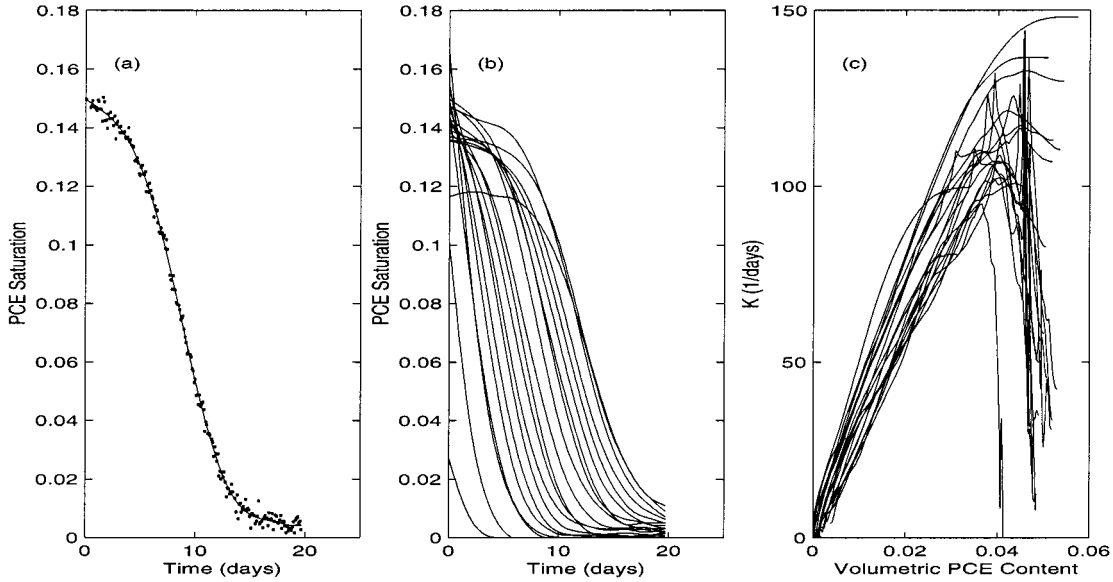

FIGURE 4. Data for experiment Water1. (a) PCE saturation at a single location, points representing measurements, the line representing a cubic tension spline fit to the data. (b) PCE saturation at every location, each line represents a different location along the column. (c) Mass transfer rate coefficient, as calculated from the saturation data.

Gamma System Data Reduction. Continuous derivatives of saturation with time are needed in the analysis, thus cubic tension splines (*28*) are used to provide local fit with global continuity for the derivatives dS_n/dt. Figure 4a shows a graph of saturation with time for one location from experiment Water1 (see Table 2), the line represents the cubic tension spine fit to the data points. Figure 4b is a graph of all of the saturation vs time data gathered for that experiment. Each line in the figure represents the data gathered for a different location along the column, where lines in the lower left part of the figure are locations near the inlet and lines near the upper right are at locations near the outlet. Obtaining values for the mass transfer rate coefficient requires solving eq 1 for *K*. An order of magnitude analysis of eq 2 shows that for the experimental conditions encountered here, the important terms are the velocity term and the mass transfer term (*8, 9*). This knowledge allows a simplification to be made yielding an analytic form for calculation of the concentration field in space and time, which is necessary to solve for *K* (*8, 9, 29*). The solution obtained for *K* is

$$K(x,t) = \left[\frac{\rho_n \phi(x) \frac{\partial S_n}{\partial t}(x,t)}{C(0,t) - \frac{\rho_n}{U}\int_0^x \phi(x') \frac{\partial S_n}{\partial t}(x',t)\,dx' - C_s} \right] \quad (6)$$

where *U* is the darcy velocity, and $C(0,t)$ is the concentration of the water at the top of the column (here $C(0,t) = 0$ for all experiments). Thus $K(x,t)$ is a function of the measured quantities $\phi(x)$, C_s, $C(0,t)$, and dS_n/dt. Figure 4c is a graph of the mass transfer rate coefficient *K* against the volumetric NAPL content, θ_n, for one experiment. The individual lines in the figure represent different locations along the column. The down turn in mass transfer rate coefficient found at high NAPL content has been explored in other work (*29, 30*) and will not be discussed further here.

Results and Discussion

Matrix of Experiments Performed. The results of seven column experiments as well as batch experiments corresponding to the concentration of surfactant used in the column experiments are presented here. All column experiments contained the same size distribution of sand. Some experiments were conducted in entirely new sand packs, while others were conducted in the same sand pack as a prior experiment. The effect of the sand pack is significant

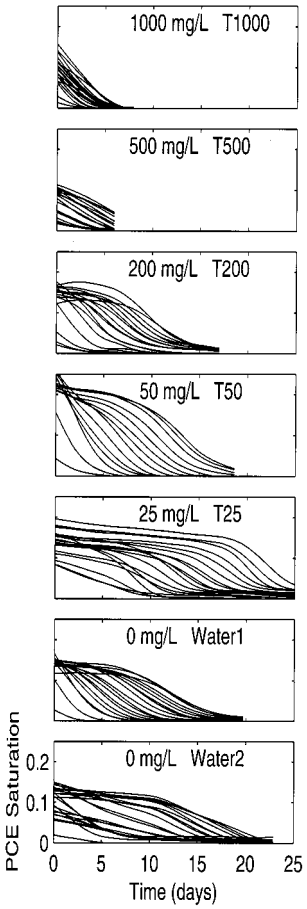

FIGURE 5. Changing saturation with time for each column experiment. Concentration of the surfactant is labeled for each experiment in mg/L. Each line represents the data from a particular column location. Each plot is on the same axes and scale.

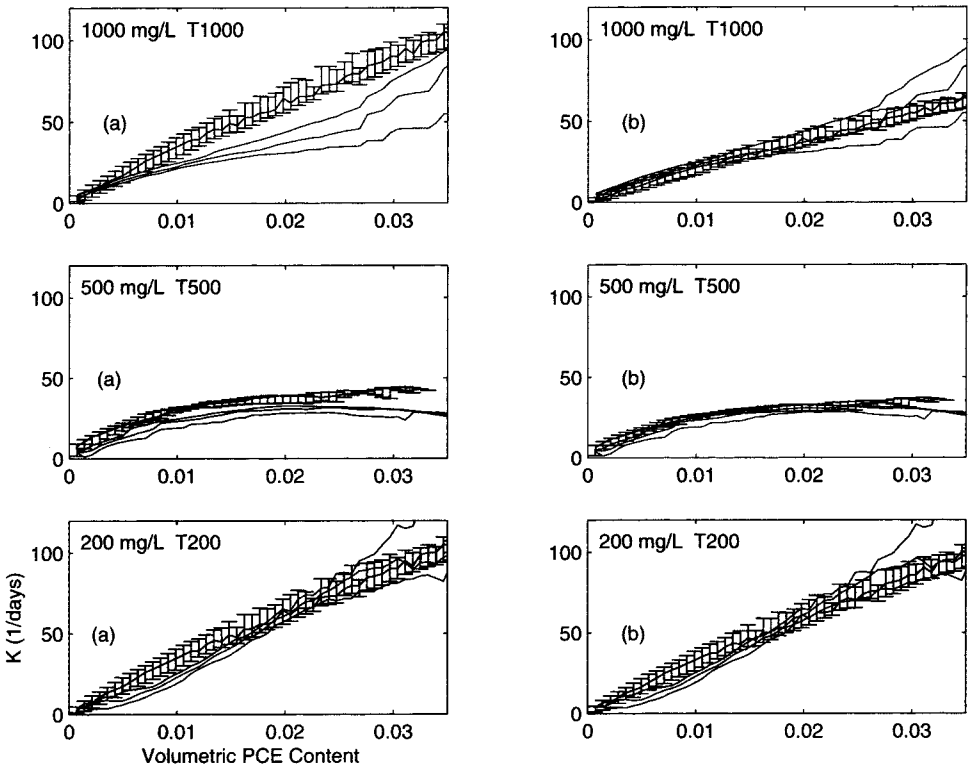

FIGURE 6. Comparison of mass transfer rate coefficients for column experiments above CMC. Concentration of the surfactant is labeled for each experiment in mg/L. Surfactant experiments are plotted as black lines representing the median, upper quartile, and lower quartile. Data based on pure water experiments are plotted as error bars representing median, upper and lower quartile. Column (a) shows an increasing disparity between $K(\theta_n)$ and $K_w(\theta_n)$ as surfactant concentration increases. Column (b) shows the resulting comparison if $K_w(\theta_n)$ is multiplied by the normalized mass transfer coefficient found from the batch experiments 0.61, 0.84, and 0.95 for surfactant concentrations 1000, 500, and 200 mg/L, respectively.

in these experiments, and analysis of the experiments relates experiments from identical sand packs where possible; alternatively the sand pack from experiment Water1 is used for comparison purposes. Table 2 lists information for each experiment including their sand pack, the amount of mass removed, and the duration of the experiment. In Table 2 the sand packs are given identification letters. Any experiment listed with this sand pack identification letter was conducted in the same column, without repacking the sand.

Figure 5 records the saturation vs time for each experiment, where each line in the figure represents data gathered from a different location in the column. The effects of the increased solubility limit can be easily seen in this figure. As surfactant concentration increases, aqueous solubility of the PCE increases as well, resulting in a decreased time for a given mass removal.

For experiments performed near and below CMC (Water1, T50, T200) there is very little difference in the mass transfer rate coefficients. This holds true despite a large change in the interfacial tension for these experiments (43.3 dynes/cm to 14.5 dynes/cm). For experiments performed above CMC (T200, T500, T1000) the values of K decreased with respect to those where the surfactant concentration is above CMC.

Each panel in Figure 6 column (a) depicts a plot of mass transfer rate against volumetric PCE content from two data sets; a surfactant enhanced dissolution data set and a pure water dissolution data set for comparison. Black lines depicting the median, upper, and lower quartiles for the data represent the surfactant enhanced dissolution data. Error bars depicting the upper and lower quartile for the data represent the pure water dissolution data. The data presented here are limited to data $0 < \theta_n < 0.035$, and only experiments above CMC are shown. The pure water dissolution experiment plotted as a comparison is one performed in the same sand pack as the surfactant enhanced dissolution experiment. A representative pure water dissolution experiment was chosen when a data set for the identical sand pack was not available (experiment T200). In each of these graphs there is a discrepancy between the pure water experiment's K and the surfactant enhanced experiment's K, the discrepancy becoming greater with increased surfactant concentration above CMC. This discrepancy in the mass transfer rate coefficient could come from either of the two components of the mass transfer rate coefficient, k or a.

Measurements of k from batch experiments can be used to predict the behavior of k in porous media experiments. Multiplying the normalized mass transfer coefficient from batch systems, k_b/k_0, by the mass transfer rate coefficient for a pure water column experiment, $K_w(\theta_n)$, gives a surrogate surfactant enhanced dissolution experiment data set. This surrogate data set assumes that the interfacial area at a particular NAPL saturation is the same for a pure water dissolution experiment as it is for a surfactant enhanced dissolution experiment. Comparing the surrogate mass transfer rate coefficient, $(k_b/k_0)K_w(\theta_n)$, to the real mass transfer rate coefficient, $K(\theta_n)$, we find a remarkable degree of similarity. Figure 6 column (b) depicts the comparison between the surrogate and the real mass transfer rate coefficient for each experiment above CMC. The test is to see if eq 7 holds true.

$$K(\theta_n) = \frac{k_b}{k_0} K_w(\theta_n) \tag{7}$$

The graphs overlap by a remarkable degree indicating that the majority of the change in the mass transfer rate coefficient, K, is directly attributable to the mass transfer

coefficient, k. The overlap also indicates that the interfacial area at any particular PCE content has not changed significantly between experiments, despite the large reduction in interfacial tension.

This result yields a practical method for prediction of mass transfer behavior of a surfactant enhanced dissolution system. It indicates that a single detailed mass transfer experiment within a porous media can be extrapolated to any surfactant by applying a correction to the mass transfer rate coefficient based on the appropriate batch experimental results. These predictions hold true for the experimental conditions examined, where NAPL saturation in the porous media is below residual and where emulsions did not form.

Modeled Results. To explore the significance of this result to application of surfactant enhanced remediation, a program was written to solve eqs 1 and 2. The equation for the transport of the dissolved phase is solved using finite differences with a variably weighted Euler scheme for the time discretization and a centered in space approximation for the spatial derivatives. The transport equation is solved first, and then the new concentration values are used to update the NAPL saturation at each time step. Concentration is set to zero at the top of the column, and diffusive flux out of the bottom is set to zero.

Simulations showed that dissolution of a 2 cm region of residual NAPL by water takes 20 days to achieve 99.9% mass removal, with a NAPL solubility limit of 250 mg/L. Adding surfactant to raise the solubility limit to 590 mg/L results in 99.9% mass removal in 8.5 days.

Current practice for estimating cleanup times follows the above procedure and ignores the effect of the surfactant on the mass transfer rate coefficient. For this simple example, correcting the mass transfer rate coefficient to 61% of its original value (from the data for experiment T1000) results in a cleanup time of 11 days, or 30% longer than originally estimated.

Acknowledgments

This research was supported by Westinghouse Savannah River Company under Subcontract AB 46396-0. The authors would like to thank the project officer, Dr. David Tuck, for his support and participation in this research.

Literature Cited

(1) Mackay, D. M.; Roberts, P. V.; Cherry, J. A. *Environ, Sci. Technol.* **1985**, *19*, 384−392.
(2) Hunt, J. R.; Sitar, N.; Udell, K. S. *Water Resour. Res.* **1988**a, *24*, 1247−1258.
(3) Hunt, J. R.; Sitar, N.; Udell, K. S. *Water Resour. Res.* **1988**b, *24*, 1259−1269.
(4) Miller, C. T.; Porier-McNiell, M. M., Mayer, A. S. *Water Resour. Res.* **1990**, *26*, 2783.
(5) Powers, S. E.; Abriola, L. M.; Weber, W. J., Jr. *Water Resour. Res.* **1992**, *28*, 2691−2705.
(6) Powers, S. E.; Abriola, L. M.; Weber, W. J., Jr. *Water Resour. Res.* **1994**, *30*, 321.
(7) Geller J. T.; Hunt J. R. *Water Resour. Res.* **1993**, *29*, 833−845.
(8) Imhoff, P. T.; Jaffé, P. R.; Pinder, G. F. *Water Resour. Res.* **1994**, *30*, 307−320.
(9) Imhoff, P. T. Ph.D. Dissertation, Princeton University, 1992.
(10) Powers, S. E.; Loureiro, C. O.; Abriola, L. M.; Weber, W. J., Jr. *Water Resour. Res.* **1991**, *27*, 463−477.
(11) Kile, D. E.; Chiou, C. T. *Environ. Sci. Technol.* **1989**, *23*, 832−838.
(12) Edwards, D. A.; Luthy, R. G.; Lin, Z. *Environ. Sci. Technol.* **1991**, *25*, 127−133.
(13) Pennell, K. D.; Pope, G. A.; Abriola, L. M. *Environ. Sci. Technol.* **1996**, *30*, 1328−1335.
(14) Pennell, K. D.; Abriola, L. M.; Weber, W. J., Jr. *Environ. Sci. Technol.* **1993**, *27*, 2332.
(15) Pennell, K. D.; Jin, M.; Abriola, L. M.; Pope, G. A. *J. Contam. Hydrol.* **1994**, *16*, 35−53.
(16) Okuda, I.; McBride, J. F.; Gleyzer, S. N.; Miller, C. T. *Environ. Sci Technol.* **1996**, *30*, 1852−1860.
(17) Fountain, J. C. Field tests of surfactant flooding. In *Transport and remediation of subsurface contaminants*; Sabatini, D. A., Knox, R. C., Eds.; ACS Symposium Series 491; American Chemical Society: Washington DC, 1992; pp 183−191.
(18) Abriola, L. M.; Dekker: T. J.; Pennell, K. D. *Environ. Sci. Technol.* **1993**, *27*, 2341−2351.
(19) Guha, S.; Jaffé P. R. *Environ. Sci. Technol.* **1996**, *30*, 1382−1391.
(20) Mills, W. B.; Porcella, D. B.; Ungs, M. J.; Gherini, S. A.; Summers, K. V.; Lingfung, M.; Rupp, G. L.; Bowie, G. L.; Haith, D. A. *Water quality assessment: A screening procedure for toxic and conventional pollutants in surface and groundwater* (Revised 1985), *Part 1*; EPA/600/6-85/002a; U.S. Environmental Protection Agency: 1985; p 19.
(21) Horvath, A. L. *Halogenated hydrocarbons solubility-miscibility with water*; Marcel Dekker Inc.: New York and Basel, 1982; p 501.
(22) Pankow, J. F.; Feenstra, S.; Cherry, J. A.; Ryan, M. K. Dense chlorinated solvents in groundwater: Background and history of the problem. In *Dense chlorinated solvents and other DNAPLs in groundwater*; Waterloo Press: Guelph, Ontario, 1996; p 14.
(23) Gosset J. M. *Environ. Sci. Technol.* **1987**, *21*, 202−208.
(24) Pankow, J. F.; Johnson R. L. Physical and chemical properties of dense nonaqueous phase liquid (DNAPL) compounds. In *Dense chlorinated solvents and other DNAPLs in groundwater*; Waterloo Press: Portland, Oregon, 1996; pp 507−512.
(25) Sun, S.; Guha, S.; Brown, D. G.; Jaffé, P. R. The effect of a surfactant's hydrophilic chain length on the surfactant-enhanced mass transfer between an organic and an aqueous phase. *I&EC Special Symposium American Chemical Society, Birmingham AL, September 9−11*, 1996.
(26) Hopmans, J. W.; Dane, J. H. *Water Resour. Res.* **1986**, *22*, 1109−1114.
(27) Ferrand, L. A.; Milly, P. C. D.; Pinder, G. F. *Water Resour. Res.* **1986**, *22*, 1657−1663.
(28) de Boor, C. *A practical guide to splines. Applied mathematical sciences*; Spinger-Verlag Inc.: New York, 1978; Vol. 27.
(29) Johnson, J. C. Ph.D. Dissertation, Princeton University, 1998.
(30) Johnson, J. C.; Jaffé, P. R. Mass transfer rate coefficients in porous media: surfactant enhanced dissolution. In *Proceedings of the 1998 symposium on environmental models and experiments envisioning tomorrow*; Chrysikopoulos, C. V., Harmon, T., Bear, J., Eds.; University of California-Irvine: 1998; pp 125−136.

Received for review September 2, 1998. Revised manuscript received February 4, 1999. Accepted February 4, 1999.

ES980908D